Dynamic Camouflage in Benthic and Pelagic Cephalopods: An Interdisciplinary Approach to Crypsis Based on Color, Reflection, and Bioluminescence

Sönke Johnsen
Biology Department
Duke University
Durham, NC 27708
phone: (919) 660-7321 fax: (919) 660-7293 email: sjohnsen@duke.edu

Alison Sweeney
Physics and Astronomy Department
U. of Pennsylvania
Philadelphia, PA 19104
phone: (215) 573-7569 fax: (215) 898-2010 email: alisonsw@physics.upenn.edu

Daniel Morse
Marine Science Institute
U. of California at Santa Barbara
Santa Barbara, CA 93106
phone: (805) 893-8982 fax: (805) 893-7998 email: d_morse@lifesci.ucsb.edu

Dariusz Stramski
Marine Physical Lab
Scripps Inst. of Oceanography, UCSD
La Jolla, CA 92093
phone: (858) 534-3353 fax: (858) 534-7641 email: dstramski@ucsd.edu

Jules Jaffe
Marine Physical Lab
Scripps Inst. of Oceanography, UCSD
La Jolla, CA 92093
phone: (858) 534-6101 fax: (858) 534-7641 email: jules@mpl.ucsd.edu

Award Number: N00014-09-1-1053
http://www.biology.duke.edu/johnsenlab

LONG-TERM GOALS

Our overall goal is to understand the perceptual and mechanistic principles that underlay camouflage framed in the context of the animals' environment. In particular, we hope to characterize and understand the perceptual abilities of several species of benthic and pelagic cephalopods, the aspects of their optical environment that affect their camouflage behavior, the

Report Documentation Page

Form Approved
OMB No. 0704-0188

1. REPORT DATE **30 SEP 2013**	2. REPORT TYPE	3. DATES COVERED **00-00-2013 to 00-00-2013**

4. TITLE AND SUBTITLE **Dynamic Camouflage in Benthic and Pelagic Cephalopods: An Interdisciplinary Approach to Crypsis Based on Color, Reflection, and Bioluminescence**	5a. CONTRACT NUMBER 5b. GRANT NUMBER 5c. PROGRAM ELEMENT NUMBER
6. AUTHOR(S)	5d. PROJECT NUMBER 5e. TASK NUMBER 5f. WORK UNIT NUMBER
7. PERFORMING ORGANIZATION NAME(S) AND ADDRESS(ES) **Duke University ,Biology Department ,Durham,NC,27708**	8. PERFORMING ORGANIZATION REPORT NUMBER
9. SPONSORING/MONITORING AGENCY NAME(S) AND ADDRESS(ES)	10. SPONSOR/MONITOR'S ACRONYM(S) 11. SPONSOR/MONITOR'S REPORT NUMBER(S)

12. DISTRIBUTION/AVAILABILITY STATEMENT
Approved for public release; distribution unlimited

13. SUPPLEMENTARY NOTES

14. ABSTRACT

15. SUBJECT TERMS

16. SECURITY CLASSIFICATION OF:			17. LIMITATION OF ABSTRACT	18. NUMBER OF PAGES	19a. NAME OF RESPONSIBLE PERSON
a. REPORT **unclassified**	b. ABSTRACT **unclassified**	c. THIS PAGE **unclassified**	**Same as Report (SAR)**	**21**	

Standard Form 298 (Rev. 8-98)
Prescribed by ANSI Std Z39-18

characterization of that behavior, and the molecular mechanisms inside the skin by which those responses are accomplished.

OBJECTIVES

1. To characterize the spatiotemporal characteristics of the near-surface and shallow benthic underwater light field, including ultraviolet radiation and polarization.

2. To determine the visual abilities of several species of cephalopod and model both the shallow and deep-water world from the animals' points of view.

3. To incorporate the knowledge gained from objectives 1 and 2 in order to study the camouflage behavior of these species under simulated ocean conditions.

4. To understand the underlying molecular and biophysical mechanisms governing changes in the skin that produce the observed optical effects, to provide a platform for future translational efforts.

APPROACH

Objective 1, Light measurements: Our approach to characterize the underwater light fields includes radiometric measurements with custom-built SQUID and Porcupine instruments and commercial hyperspectral sensors from TriOS(Germany) and Satlantic (Canada). SQUID (SeQuence of Underwater Irradiance Detectors) was developed for this project to provide a unique capability to measure both spatial and temporal statistical properties of downwelling irradiance fluctuations produced by surface-wave focusing within the surface ocean layer. The Porcupine instrument was developed for the ONR RaDyO program to measure temporal properties of high-frequency fluctuations in downwelling radiance and irradiance at several light wavelengths, and it complements SQUID measurements in this project. Both SQUID and Porcupine provide light measurements with a high sampling rate of 1 kHz. The TriOS and Satlantic sensors provide measurements of irradiance and radiance with an averaging time typically from about 0.002 to >1 s (depending on light intensity) and with high spectral resolution (~3 nm from 350 to 850 nm). Radiative transfer simulations are also used in this project as an additional tool to characterize the underwater light field.

Objective 2, visual physiology: our approach involves using microscopy, microspectrophotometry and the optomotor response to measure six primary visual parameters of the study species: field of view, spectral sensitivity, acuity, temporal resolution, and contrast and polarization sensitivity. Field of view is determined from the placement and orientation of the eyes and the geometry of the retina and pupil. Spectral sensitivity will be investigated using microspectrophotometry (MSP), which measures the absorption spectra of individual photoreceptors. Spatial and temporal resolution will be estimated from the spacing of photoreceptors in the retina and via the optomotor response. Contrast sensitivity is estimated by determining photon catch and also via optomotor assays using stripes of decreasing contrast. Polarization sensitivity will also be assayed via retinal morphology and optomotor response.

Objective 3, camouflage behavior: Camouflage behavior is studied both *in situ* and within various controlled environments, including a "holodeck", a tank surrounded by monitors that project natural environments or controlled visual stimuli. The top of the tank has a plexiglass "floatee" that will make the surface optically flat and permit undistorted observation of the animals from the outside as well as permitting images to be projected into the tank by two DLP projection systems.

Objective 4, biophotonics: We will characterize the optics of the skin using fiber-optic spectroscopy coupled with goniometry, measuring the polarization-specific bidirectional reflectance of the skin of the target species and correlate these with the statistical analyses of the light measurements from objective 1 to determine which aspects of this complex reflectance have specifically evolved for camouflage. We will also determine the ultrastructure of the reflectin-based structures using transmission electron microscopy and model their optical effects to determine what aspects of the biological structures are important for the observed environmental optical match. We will also investigate the biophysical mechanisms governing tunable, self-assembling reflectance.

WORK COMPLETED

Objective 1, Light measurements: During the reporting period we have completed two major new tasks: (i) analysis of data of horizontal spectral radiance collected on the KM12-10 cruise in the Pacific waters off Hawaii Islands, and (ii) radiative transfer simulations of light field in the mesopelagic zone of the ocean and the analysis of data from these simulations. Unique radiometric data collected during the KM12-10 cruise included vertical profiles of horizontal radiance from two opposite directions within the principal solar plane, which were taken at different solar angles. The results from our analysis of these data are part of the collaborative manuscript led by Sönke Johnsen with participation of the Stramski team (Johnsen et al., in prep). The Stramski team is also working on a separate manuscript with the sole focus on the optical aspects of horizontal light field in the upper ocean. In this effort we use both the radiance data from the KM12-10 cruise and the "horizontal" measurements of scalar and plane irradiances which we collected during the earlier project-sponsored cruise in the Gulf of California in 2010. With regard to our second task, we have undertaken this work to provide a unique comprehensive characterization of natural light field within the mesopelagic zone. This task was completed and the manuscript was submitted for publication (Li et al., in review). We also continued the analysis of power spectra of wave-induced light fluctuations at near-surface depths in the ocean under sunny conditions. The results from this analysis were presented at the Ocean Optics XXI Conference in Glasgow in October 2012 (Sawicka et al., 2012) and the manuscript is in preparation (Gassmann et al, in prep.).

The Omnicam instrument was reconfigured to maximize sensitivity for deep-sea ambient light measurements. By reconfiguring the camera parameters, it was possible to increase low light sensitivity. Although the captured images had decreased resolution, this allowed for ambient light to be measured deeper than previously possible. Tests were performed off SIO pier and field deployments were on *R/V New Horizon.* Based on the field study results, a comparative analysis of highly sensitive detectors was performed. Hardware reconfiguration of Omnicam will allow for measurement of quantum irradiance (photon counts). Estimates from radiative transfer simulations show that we can reliably measure down to 500 m and potentially as deep as 1000 m, depending on environmental conditions.

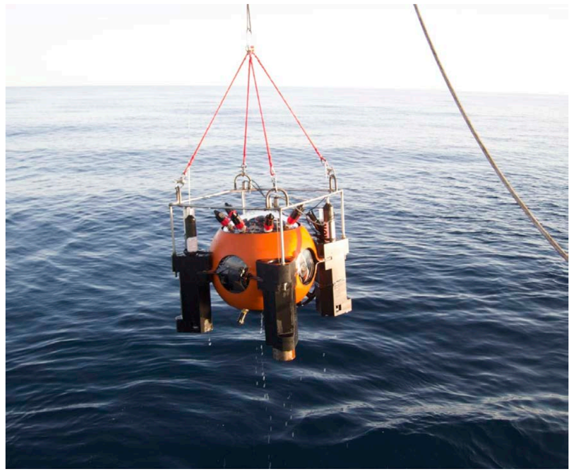

Figure 1: Omnicam deep-sea configuration during New Horizon deployments.

Deep-sea light measurements: The software reconfigured Omnicam was deployed off the coast of San Diego on the *R/V New Horizon* in April 2013, as shown in Figure 1. Three test deployments were performed down to 1000 m to assess the current capabilities of the instrument and to guide future deep-sea configurations.

Objectives 2 and 3, visual physiology and camouflage behavior: Many cephalopods change color while they attack prey. We have begun data collection for behavioral studies investigating the possibility that this color change confuses prey, acting to camouflage attack motion. Figure 2B shows how brief squid, *Lolliguncula brevis,* change color through time points 1, 2, and 3 of an attack. We are testing whether this sequence changes the grass shrimp *Palaemonetes'* escape response relative to controls with no color change (figure 2A and 2C). We are beginning to assess color change attack strategies in other cephalopod species. We have collected preliminary data for behavioral studies of cuttlefish camouflage strategies. Data will begin to define the elicitation space for camouflage patterns, or the spatial area over which environmental stimuli influence camouflage response (figure 3). This initial work will assess the elicitation space for very basic camouflage pattern components responding to simple environmental stimuli. Data will also assess whether camouflage strategies respond to spatial and temporal abundance of features in the environment, by testing whether cuttlefish preferentially match common rather than rare objects in the environment. We have also conducted a comprehensive review of the role of proportion-based perception in animals and how this is predicted to influence the evolution of behavioral signaling and sensory scene analysis (Akre and Johnsen, in prep).

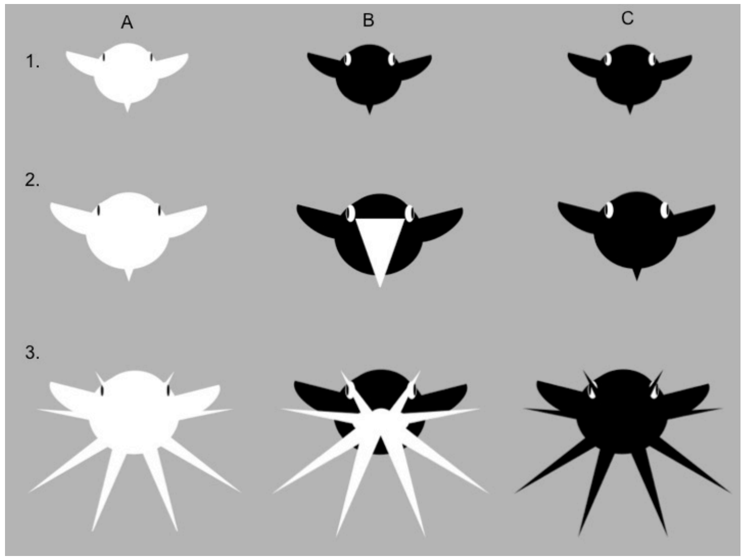

Figure 2: Some cephalopods change color during attack. Column B shows sequence of color change during Lolliguncula brevis attack through time points 1, 2, and 3. Controls are shown in columns A and C.

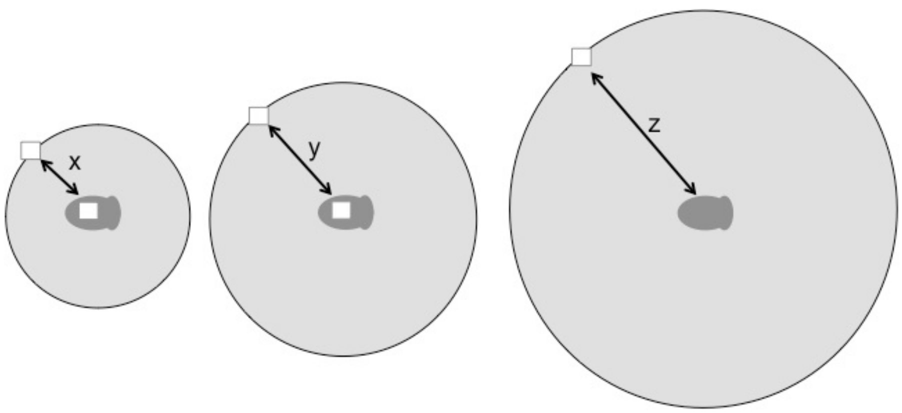

Figure 3: Camouflage patterns are elicited by environmental features. To determine the elicitation distance for the white square component of this cuttlefish pattern, we can measure the distance from which a white rock elicits the pattern. Here, y < elicitation distance < z.

Bioelectric crypsis: Body movements and ion exchange at the gills in cuttlefish, *Sepia officinalis*, are associated with ventilation and act as both visual (motion) and electric stimuli for electrosensitive predators. The signals are modulated to decrease detection by predators in response to a predator-simulating stimulus. Motion and bioelectric stimuli were recorded from *S. officinalis* in response to a looming fish predator stimulus (figure 4). The DC electric stimuli recorded from *S. officinalis* during rest, freeze (predator-avoidance response), and jet (escape) behaviors were used in a behavioral assay to quantify bonnethead shark, *Sphyrna tiburo*, and blacktip shark, *Carcharhinus limbatus*, responses to electric fields associated with these different behaviors.

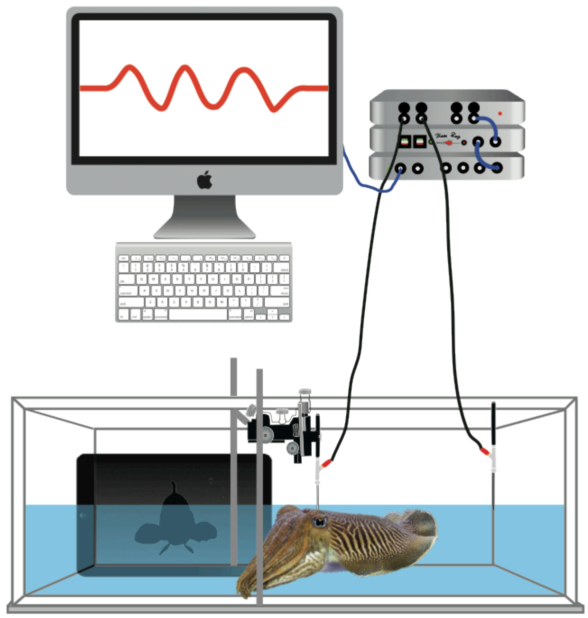

Figure 4. Experimental set-up for recording behavioral and physiological responses of cuttlefish, Sepia officinalis, to a looming predator stimulus. A video of a looming fish predator was played on an iPad positioned along one wall of an experimental tank. Behavior (body movement from ventilation) and bioelectric field responses (associated with ion exchange during ventilation) were recorded over the course of the predator simulation with video cameras and a recording electrode positioned at the opening of the mantle.

Objective 4, biophotonics and instrumentation development: We completed our elucidation of the ultrastructural basis and unifying biophysical mechanism controlling the dynamically tunable "structural color" and the switchable, omnidirectional white produced by the reflective iridocytes and leucophores in cephalopod skin. In addition to discovering the unification of the underlying mechanism of these two dynamically controllable biophotonic systems, our work provides new insights into the principles of camouflage for moving objects and edge-disruption in "caustic" light environments.

RESULTS

Objective 1, Light measurements: In this report we present example results from radiative transfer simulations of the solar light field in the mesopelagic zone (depth range 200 - 1000 m). These simulations were performed for several scenarios of surface boundary conditions and inherent optical properties within the ocean surface layer which provided, for the first time, a comprehensive characterization of variations in the magnitude, spectral composition, and angular distribution of various radiometric quantities of the solar light field as well as the behavior of apparent optical properties (AOPs) within the entire mesopelagic zone across the entire visible spectrum of light. Figure 5 illustrates a very large dynamic range of irradiance within the mesopelagic zone as well as the dominant contribution of inelastic radiative processes to the mesopelagic light at wavelengths longer than 500 nm. The spectral values of scalar irradiance decrease typically by about 9-10 orders of magnitude between the top and bottom of the mesopelagic zone. Ignoring the presence of inelastic processes in the ocean yields totally unrealistic results in the green and red portions of the spectrum but

has small or negligible effect in the blue. Raman scattering by water molecules plays the most important role among the inelastic processes but the effects of fluorescence of CDOM at mesopelagic depths are also significant. Figure 6 shows that the angular distribution of mesopelagic light is dramatically different at different light wavelengths. In the blue, the radiance distribution at mesopelagic depths all the way down to 1000 m is dominated by downwelling light. In contrast, in the red the radiance distribution is nearly uniform, which is caused by the contributions of inelastic processes. A closer inspection of such radiance data reveals that the shape of the angular distribution of light remains nearly unchanged throughout the deeper portion of the mesopelagic zone (below approximately 400 - 500 m), implying that the light field reached the asymptotic regime. The results for the AOPs support this conclusion. Figure 7 shows spectra of three example AOPs, the average cosine of total light field, diffuse attenuation coefficient of downward plane irradiance, and irradiance reflectance. For all three cases the spectra of these AOPs converge on one another for the example mesopelagic depths of 500, 800, and 1000 m. This comprehensive characterization of the mesopelagic light field accomplished through radiative transfer simulations is expected to benefit studies of vision and crypsis of mesopelagic animals and serve as a reference for interpretation of deep-sea measurements with the Omnicam instrument.

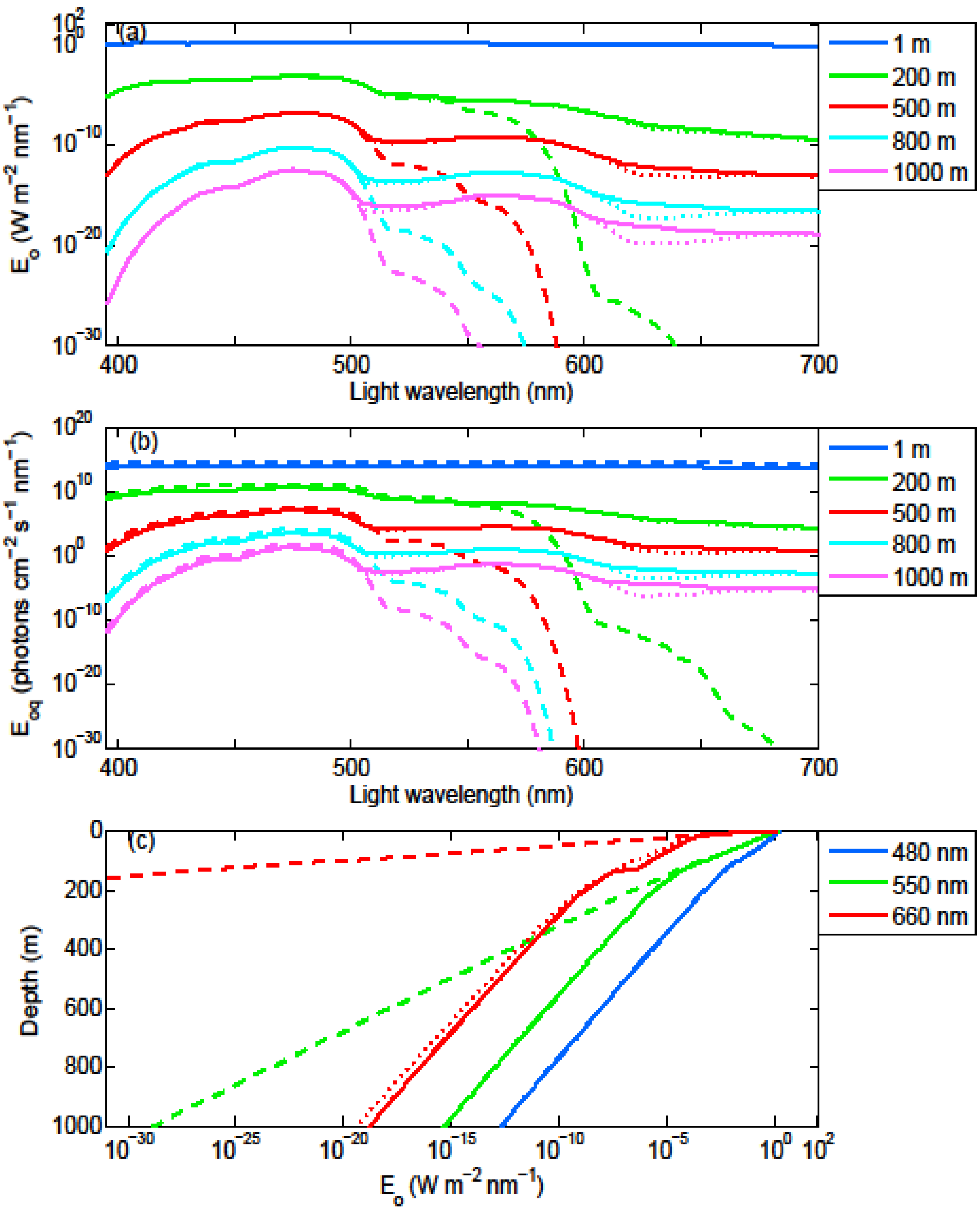

Figure 5 (a): Spectra of scalar irradiance E_o for selected depths as indicated; (b): Spectra of quantum scalar irradiance E_{oq} derived from E_o presented in panel (a); (c): Depth profiles of E_o for selected light wavelengths as indicated. Dashed lines represent radiative transfer simulations with no inelastic radiative processes; dotted lines represent simulations with Raman scattering by water molecules included; and dashed lines represent simulations with Raman scattering and fluorescence of CDOM and chlorophyll-a included. These results were obtained for clear sky conditions with solar zenith angle of 30^o and the chlorophyll-a concentration in the surface layer Chl = 0.2 mg m^{-3}.

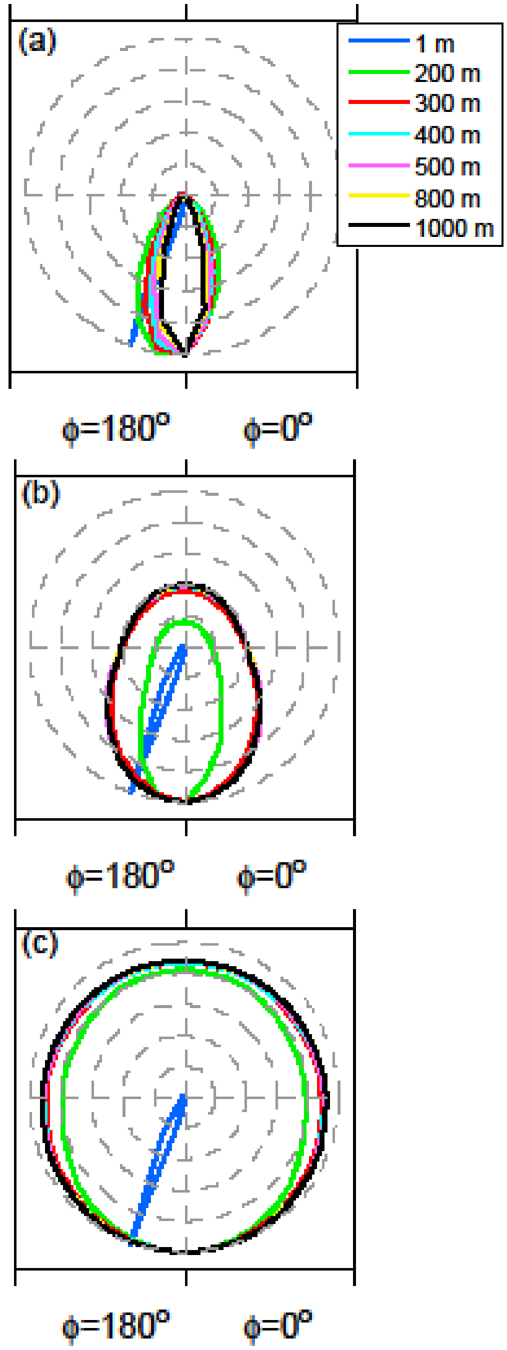

Figure 6: Diagrams illustrating the shape of the angular distribution of radiance at three selected wavelengths, 480 nm (panel a), 550 nm (panel b), and 660 nm (panel c) for selected depths as indicated. To facilitate a comparison of shapes the radiance values of each distribution were normalized by the maximum value of radiance. The distributions are within the solar principal plane. The right half of the plane denoted as $\phi = 0^o$ contains the sun. The left half of the plane denoted as $\phi = 180^o$ is the opposite part of the solar principal plane. These results were obtained from simulations for clear sky conditions, solar zenith angle of 30^o, and the chlorophyll-a concentration in the surface layer Chl = 0.2 mg m^{-3}. The inelastic radiative processes were included in the simulations.

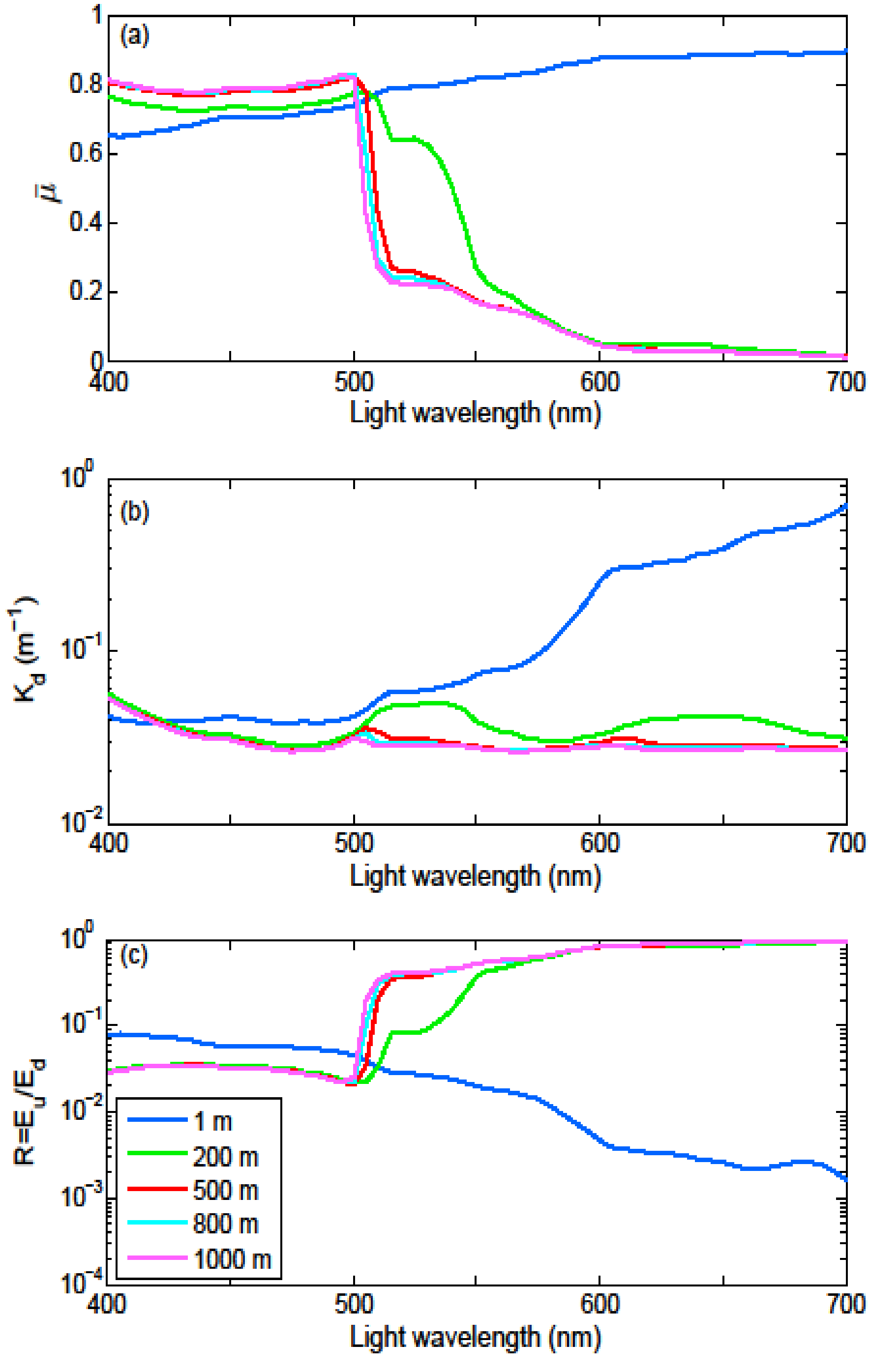

Figure 7: Spectra of apparent optical properties of the ocean at selected depths as indicated. (a) Average cosine of the total light field; (b) Diffuse attenuation coefficient for the downward plane irradiance; and (c) Irradiance reflectance. These results were obtained from simulations for clear sky conditions, solar zenith angle of 30^o, and the chlorophyll-a concentration in the surface layer Chl = 0.2 mg m^{-3}. The inelastic radiative processes were included in the simulations.

Deep-sea light measurements: Example measurements are shown in Figure 8 for average light intensity at the six different directions accessible by the Omnicam instrument. It is apparent that the maximum depth for light detection with the current Omnicam hardware configuration is approximately 250 m. The results clearly indicate that detector sensitivity must be increased if we are to reach 1000 m depth.

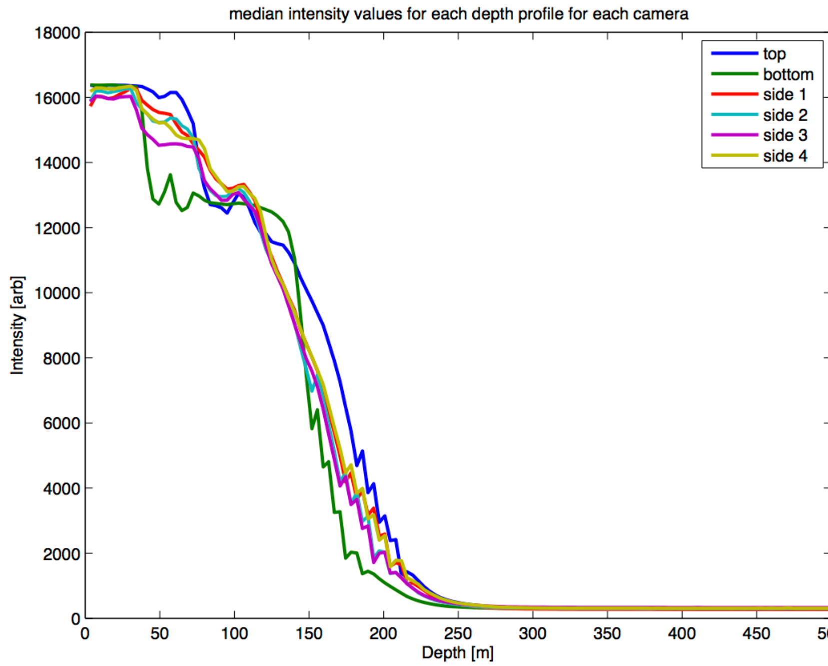

Figure 8: Preliminary results from Omnicam deep-sea deployments.

The ultra low light sensitive detector that has been selected is the Hamamatsu multi-pixel photon counter (MPPC) module C11208-03. This detector consists of an array of silicon avalanche photodiodes and will allow for photon counts down to 1000 m depth. The MPPC spectral response peak is 440nm, which is quite close to the 480nm spectral peak of light in the ocean. Measurements will be made using a spectral filter centered at 480nm with 20nm bandwidth. Photon counts will be converted to quantum irradiance quantities and compared with the results of radiative transfer simulations from the Stramski group (SIO/UCSD). A research cruise for Omnicam deployment on the *R/V Robert Gordon Sproul* is scheduled for late fall 2013. Additional deployments of opportunity will also be sought, in order to obtain as geographically and temporally diverse a data set as possible.

BRDF measurements: A paper on the optical scatterometer for measurement of angular reflectance (OSMAR) instrument was published (Haag et al., 2013). The results presented therein correspond to a limited selection of the bidirectional reflectance distribution function (BRDF) data set collected from the 2012 *R/V Kilo Moana* research cruise off the Hawaiian Islands. Full processing algorithms were completed for the BRDF data in early 2013. For proper analysis of the data, geometric distortion correction, multiple exposure integration, and normal estimation are key aspects that must be considered. An example result from the full processing algorithm, including multiple exposure integration, is shown in Figure 9. Note that there is more intensity information in each processed BRDF map than can generally be displayed on a standard computer screen.

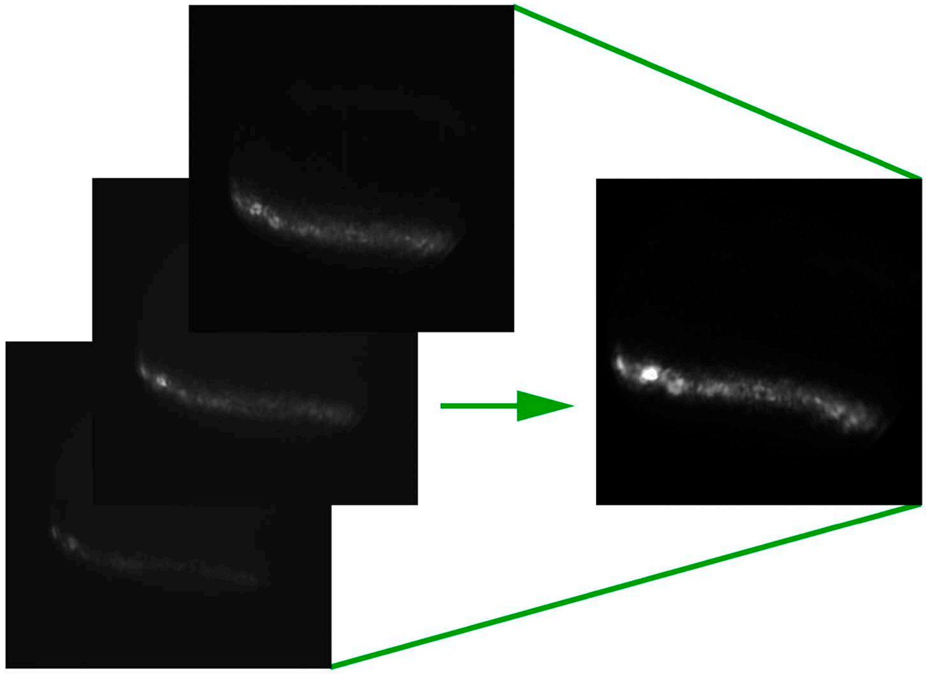

Figure 9: Example result from full BRDF data processing algorithm.

Continuing efforts are focused on the development of models that will allow for generalization of BRDFs for individual species. That is, we suppose a given species has a limited range of scattering patterns and postulate that we can derive reasonably simple parametric models from the collected data set. Once completed, the BRDF models will be compared with the results of transmission electron microscopy (TEM) performed on fixed animal specimens and subsequent physical scattering models, in collaboration with the Sweeney (UPenn) group.

Objectives 2 and 3, visual physiology and camouflage behavior: Sepia officinalis decreased motion and bioelectric stimuli in response to an approaching predator stimulus (figure 10). The amplitude of body movements and voltage was decreased by 71% and 37%, respectively, at the onset of the stimulus. The frequency of body movements and the bioelectric field were reduced by 54% and 51%, respectively. Bonnethead and blacktip sharks responded to the jetting stimulus (200µV) significantly more than the resting stimulus (30µV) (figure 11). Sharks responded to the freeze stimulus (10µV) significantly less than jetting and resting stimuli (P<0.0001). Detection of electric stimulus is distance dependent and larger electric fields are detected at a greater distance. The detection distance of bonnethead sharks with an electrosensitivity of 50nV cm^{-1} was calculated for each *S. officinalis*-simulating stimulus (figure 12). The freeze response decreases detection distance by 1.5cm relative to the resting stimulus, whereas the jetting stimulus increases detection distance by 15cm. These results suggest that cuttlefish may experience a decrease in predation risk by reducing motion and electric stimuli used by foraging shark predators.

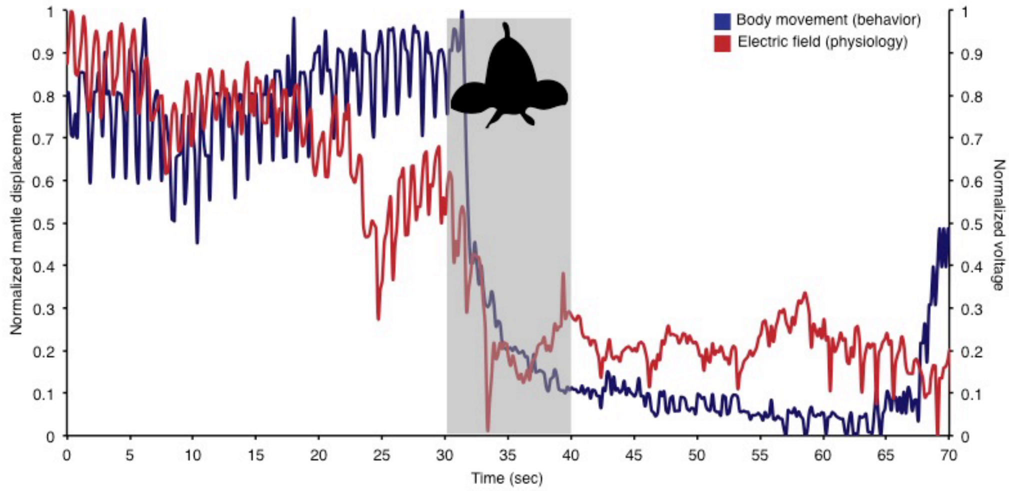

Figure 10. Normalized behavioral (blue) and physiological (red) responses of Sepia officinalis to a looming predator stimulus. The amplitude and frequency of body movements associated with ventilation were reduced at the onset of the predator stimulus and remained reduced for up to 1min past the retreat of the stimulus.

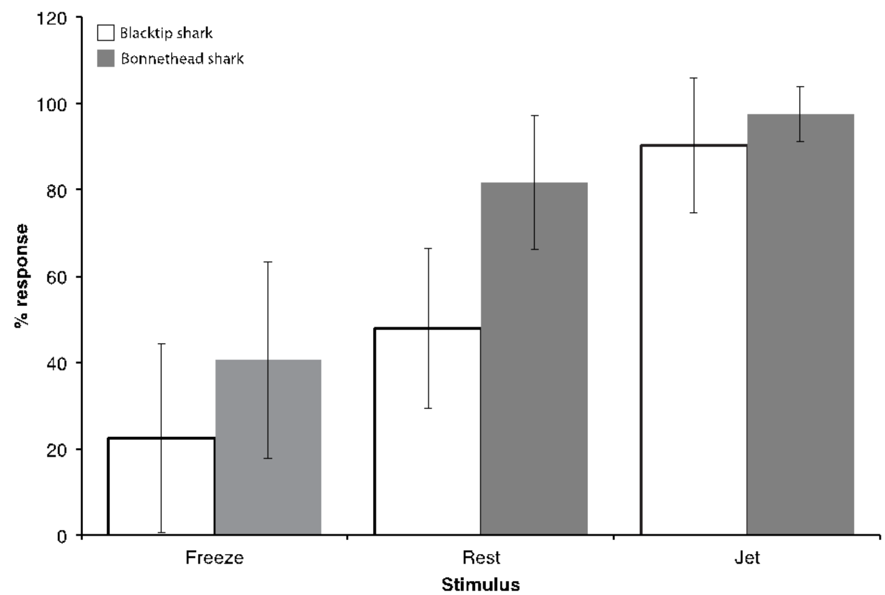

Figure 11. Mean proportion (± SD) of shark responses to each cuttlefish electric stimulus. Sharks responded to the freeze magnitude stimulus significantly less frequently than the resting and jetting stimulus (P<0.0001). Open bars are blacktip sharks and solid bars are bonnethead sharks.

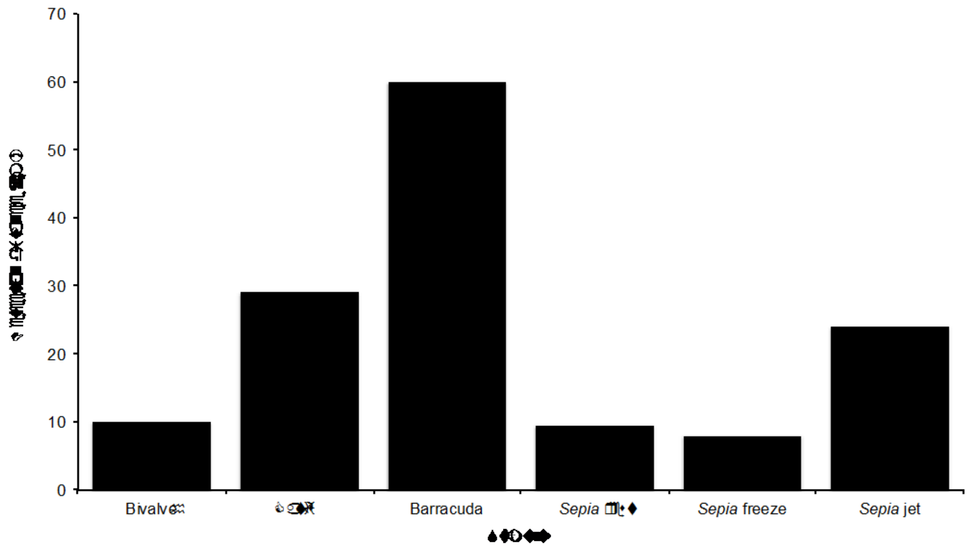

Figure 12. Theorectical detection distance (cm) for bonnethead sharks, Sphyrna tiburo, to prey with different magnitude bioelectric fields. Prey with larger electric fields are detectable at a greater distance. Cuttlefish, Sepia officinalis, are within the detection range for bonnethead sharks at 9.5cm when resting. Detection decreases to 8cm in cuttlefish demonstrating a freeze response and increases to 24cm for cuttlefish that demonstrate escape (jet) responses to a predator stimulus.

Objective 4, biophotonics: Dariusz Stramski (co-leader of our MURI's SIO team) showed that the flicker intensity varies by as much as ca. 100-fold in highly "caustic" daytime shallow-water environments. Key to the camouflage of moving objects and edge-disruption in such light environments is the display of patterned white reflectance (Figure 13).

Figure 13. Patterned reflectance of white yields effective camouflage for moving objects and effective edge-disruption in caustic shallow-water light environments.

The UCSB team completed its elucidation of the origin and ultrastructure of the lamellar Bragg reflectors that yield tunable colored reflectance from the iridocytes in cephalopod skin, using focused ion beam dissection of these cells and electron microscopy to prove unequivocally that the Bragg lamellae are formed by repeated invaginations of the cell membrane (Figure 14).

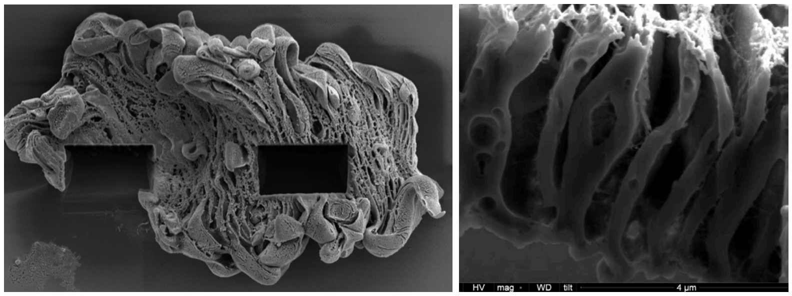

Figure 14. (left) Focused ion beam was used to expose cross sections of the tunable iridocytes from squid skin. (right) TEM analyses of the cut sections showed unequivocally that the Bragg lamellae are formed by repeated invaginations of the cell membrane.

The significance of this finding is the discovery of the very high surface area interface between all parts of the tunable Bragg reflector in immediate contact with the external environment, explaining both the rapid and uniform response to the neurotransmitter signal activating reflectance, and the rapid, reversible expulsion and re-uptake of water across the Bragg lamellar membrane, permitting rapid changes in the thickness and spacing of the lamellae that tune its reflectance. This rapid and reversible dehydration was demonstrated using D_2O as a tracer. The reflectin proteins are the key, as we have shown that the ACh-induced signal transduction cascade culminating in changes in phosphorylation of the reflectins overcomes the Coulombic repulsion of these proteins that fill the Bragg lamellae, thus shielding their surface charges. This drives an efflux of small ions to maintain electro-osmotic equilibrium across the membranes, subsequently driving the Gibbs-Donnan expulsion of water to maintain osmotic equilibrium. While the condensation of the reflectins increases the refractive index within the lamellae, thus activating Bragg reflectance, the dehydration changing the thickness and spacing of the lamellae shifts the color of the reflected light across the entire visible spectrum.

These findings were fully verified by the first-ever microspectrophotometric analyses of this system at the sub-cellular level, allowing ***independent measurement*** of the parameters of the Bragg reflectors. While the refractive index in the lamellae increased from 1.35 to 1.48, a reduction in the thickness and spacing of the lamellae by ca. 85-115 micrometers proved sufficient to account for the entire excursion of reflectance from red to blue.

We discovered the first known population of switchable white-reflecting “leucophores” cells, and found that they operate by a mechanism essentially identical to that of the tunable color iridocytes. But in these cells, the reflectins are contained in ca. 1,000 small membrane-enclosed vesicles – rather than the lamellae of an organized Bragg reflector. ACh-activated condensation of the reflectins in these vesicles, and consequent dehydration and shrinkage of the vesicles, activates their omni-directional, broadband white reflectance – operating by the mechanism of Mie reflectance (rather than Bragg reflectance). We are working now both to explore the interconvertability of the biophotonic Bragg and Mie reflective systems, and to harness the mechanism of switchable white reflectance we discovered to develop electrically switchable, polymer-based materials.

Our work on photonic camouflage in deep-sea squids also led us to consider the reflectin-like system in giant clams. This inquiry led to a remarkable discovery of a solar energy harvesting - full optical characterization of a system that will allow efficient harvesting of photons in a low surface area, damage-resistant system. This system consists of photosynthetically active dinoflagellates organized into micropillars within the clam’s mantle tissue, and wavelength-dependent iridocyte scattering cells

that interact with these pillars to redistribute photosynthetically efficient light evenly among cells and deep into the tissue. We characterized the clam system using micron-scale intra-tissue radiometry and optical modeling, and found that this multi-scale system results in a five-fold increase in light reaching dinoflagellates compared to the same number of cells organized in a simple layer (figure 15). The evolved photonic system in the clam may present new strategies for more efficient, damage-resistant polymer-based photovoltaic devices and sunlit, spatially efficient algal biofuel production.

Our work on reflectin-based tissue transcriptomes and characterization of the structures they make has progressed. We completed mass spec confirmation of the reflectin protein composition of deep-sea reflectin-based tissues to verify the valid transcripts in our reflectin transcriptomes due to over-prediction of reflectin genes in the transcriptome assembler. In our test tissue of the eye reflector of *Dosidicus gigas*, a pilot MS/MS sequencing effort has identified approximately 60% of the mass of the tissue to be composed of reflectin proteins, and all these transcripts are present in the transcriptomes we generated. Therefore, mass spectroscopy will allow us to solve the problem of overprediction present in our transcriptome data due to the tandem repetitive nature of reflectin proteins.

On the front of novel optical functions in reflectin-based tissues, we have begun a finite-difference time domain model of the light-guiding reflectin-based structures found covering the eye of the squid *Galiteuthis*. These tissues are reflectin-based and MS/MS sequencing of major protein bands in SDS-PAGE demonstrates presence of sequences in libraries.

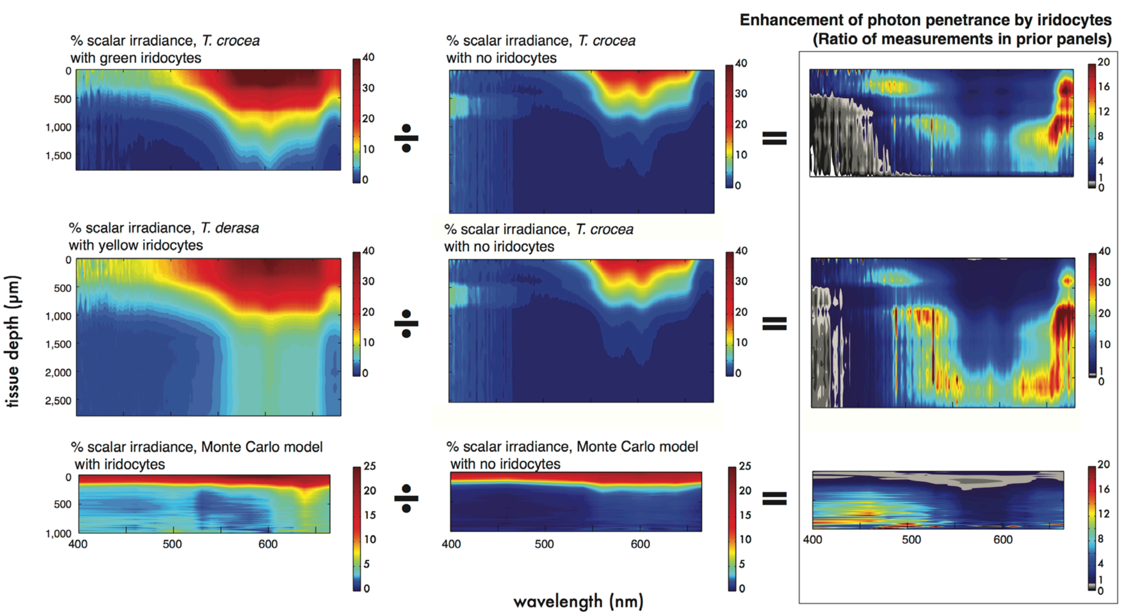

Figure 15. Optical performance of giant clams with and without iridocytes, and a Monte Carlo optical model recapitulating this performance, showing enhanced scalar irradiance.

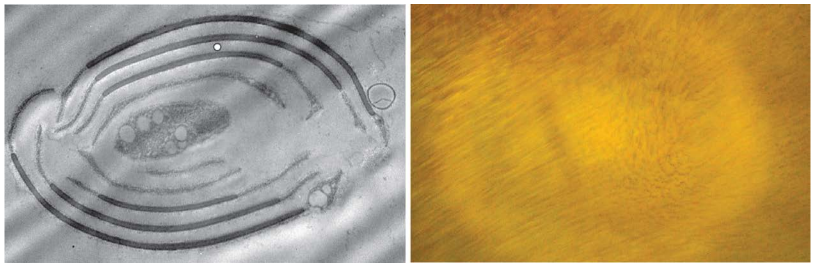

Figure 16. Left panel: Cross-section of hollow-core Bragg fiber. The fiber cross-sectional ellipticity increases propagation efficiency. Right panel: Reflectance micrograph of laminated hollow-core fibers turning to point ventrally from the bottom of the eye photophore

We have also initiated a study of the long-wavelength reflecting structures present in squid skin (such as in *Loligo opalescens*, *Chiroteuthis dux*, *Pterygioteuthis lampas*, and *Dosidicus gigas*) (figure 16). Our initial models suggest that the predominantly long-wave (600 – 700 nm) reflectance of these structures may provide good camouflage against Raman-scattered light and photons from chlorophyll fluorescence in the ocean.

IMPACT/APPLICATIONS

The systems evolved by marine animals in order to hunt, hide, and mate over hundreds of million years surpass our contemporary engineering designs for underwater vehicles. Hiding and hunting are natural tasks for our military and we believe that valuable clues will be provided by the results of our studies. The impact will hopefully affect all branches of the armed forces that have aquatic missions. This includes Special Forces, mine hunting vehicles, the submarine community, and a newest generation of underwater vehicles that could all benefit from the option of "stealth". Since visual methods play an important role in the mission profiles of all of these groups, the ability to enhance and hide from detection should be an important payoff.

The discoveries reported above point to simple new methods to achieve effective camouflage for moving objects and effective edge disruption in shallow-water and caustic day-time light environments. We have been working in close collaboration with partners at Raytheon Vision Systems Inc. since the start of this project, seeking to develop practical translations of the signature management and other useful technologies, materials and devices important to industry, the Navy and other units of DoD. Our focus is to develop low-power electrically switchable polymer-based materials for these purposes. Through this collaboration we have developed a prototype biologically inspired, lightweight, electrically switchable, polymer-based shutter for IR detectors that can be extended to coded apertures for IR imaging without a lens and to signature management in the IR (cf. patent awarded last year). In addition, the giant clam system may suggest novel geometries for devices for solar energy harvesting.

TRANSLATIONS

(**1) Electrically switchable, polymer-based shutters for IR detectors:** As described in our report, we discovered the molecular structures and mechanisms responsible for the dynamically tunable reflectance in skin cells of the squid, and are now working with Raytheon Vision Systems Inc. (with support from ARL and DARPA) to translate these finding to develop a prototype electrically

switchable, polymer-based shutter for infrared detectors. Using solution-processable conjugated polymers, we developed working prototypes that are activated by low voltage (2-3 V) to display significant changes in absorption and reflection in the IR. As the polymer-based materials transition from semiconducting to conducting, free carriers and conformational changes absorb and scatter broad bands of infrared radiation. The resulting change in refractive index resulting from the simultaneous production of absorbing species and their increased density closely parallels the synergistic simultaneous changes in the reflectin-based Bragg layers that provide the high gain exhibited by the biological system. Defense applications include noiseless IR shutters for forward Special Forces operations, graded neutral density and tunable hyperspectral IR filters, apertures, and lightweight coded apertures for IR image formation without a lens.

(**2) <u>Broadband, omnidirectional IR reflectors</u>:** Also as described above, we recently discovered that the silver, broadband reflective tissue surrounding the eyes of the squid (providing omnidirectional camouflage of that structure) is composed of a unique array of reflectin-filled, spindle-shaped cells densely packed together to form an unusual, quasi-disordered, "distributed Bragg reflector." The optical contrast between the high refractive index within these reflectin-packed cells and the low refractive index in the extracellular medium is responsible for the very high reflectivity of the tissue, while the infinite number of spacings between the nested, tapered cells in the quasi-disordered array is responsible for the broadband (i.e., multi-wavelength, silver) and omnidirectional reflection. Translating the underlying principles found in this biological broadband reflector (in research supported by ARO and Acumen, Inc.), we produced prototype broadband reflective coatings by evaporative self-assembly of asymmetric polymer rods to form quasi-disordered and "distributed" Bragg reflectors. The dimensions of the quasi-ordered polystyrene rods are sufficiently large to ensure that reflectance occurs in the IR, while the random quasi-disorder of the film ensures omnidirectionality of the reflectance. Silica and silicone casts of these organic films retain the optical properties in a rugged form suitable for device manufacture. Because the biologically inspired fabrication process is facile, error-tolerant and inexpensive and can be scaled to larger, flexible and curved surfaces; because silica and silicone casts preserve the desired optical features in a robust form suitable for manufacture of coatings; and because the optical and IR properties of those coating can be readily tuned, they offer numerous applications of potential importance to ONR and other branches of DoD.

RELATED PROJECTS

"Bioinspired Dynamically Tunable Polymer-Based Filters for Multi-Spectral Infrared Imaging"; DARPA; W911NF-08-1-0494; $150,000; 10-01/08-09/30/09. This work represents a "translation" of what we learned from the biomolecular mechanisms governing dynamically tunable reflectance in cephalopods to novel routes for synthetic optical materials. Performed in collaboration with Raytheon, Inc. This funding has ended; proposal for continuation is pending.

"Bio-inspired Visual Information Processing and Dynamically Tunable Multispectral IR Detection: Learning from the Octopus." ARL/ARO; W911NF-09-D-0001; $200,000; 1/1/09-12/31/09. To D.E. Morse and R. N. Hanlon. This work represents a "translation" of what we learned from the biomolecular mechanisms governing dynamically tunable reflectance in cephalopods to novel routes for synthetic optical materials. This funding has ended.

"Bio-Inspired Photonics: Polymer-Based, Dynamically Tunable Multi-Spectral Filters for IR Detection"; DARPA; proposal pending for continuation of effort described immediately above. This work represents a "translation" of what we learned from the biomolecular mechanisms

governing dynamically tunable reflectance in cephalopods to novel routes for synthetic optical materials.

PUBLICATIONS (from project to date)

Akre, K. L. and Johnsen, S. (in prep). Psychophysics and the evolution of behavior. *Trends in Ecology and Evolution*

Bedore, C.N., Kajiura, S.M., and Johnsen, S. (in prep). Bioelectric crypsis in a cephalopod, *Sepia officinalis*, reduces detection by shark predators.

DeMartini, D.G., A. Ghoshal, E. Eck and D.E. Morse (in prep). Discovery of tunable leucocytes, and a unified mechanism governing tunable biophotonics in squid.

DeMartini, D. G., A.M. Sweeney, J. Lew and D.E. Morse (in prep). Phosphorylation of native and recombinant squid skin reflectins in vivo and in vitro.

DeMartini, D.G., A. Ghoshal, E. Pandolfi, A.T. Weaver, M. Baum, and D.E. Morse. 2013. Dynamic Biophotonics: Female Squid Exhibit Sexually Dimorphic Tunable Leucophores and Iridocytes. *J. Exp. Biol.* **216**: 3733-3741.

DeMartini, D.V. Krogstad and D. E. Morse. 2013. Membrane invaginations facilitate reversible water flux driving tunable iridescence in a dynamic biophotonic system. *Proc. Natl. Acad. Sci. USA* **110**: 2552-2556

DeMartini, D. G., A.M. Sweeney, and D.E. Morse (in prep). Phosphorylation of native and recombinant squid skin reflectins in vivo and in vitro.

Gagnon, Y. L., Sutton, T. T., and S. Johnsen (2013). Visual acuity in pelagic fishes and mollusks. *Vision Research* **92**, 1-9.

Gassmann, E., Stramski, D., Darecki, M., and Dubranna, J. (in prep). Power spectra of wave-induced fluctuations in downward irradiance within the near-surface ocean under sunny conditions.

Ghoshal, A., D. G. DeMartini, E. Eck, and D.E. Morse (2013). Optical Parameters of the Tunable Bragg Reflectors in Squid. *J. R. Soc. Interface* **10**:

Haag, J. M., Jaffe, J. S., and Sweeney, A. M. (2013). Measurement system for marine animal reflectance functions. *Optics Express* **21(3)**, 3603-3616.

Haag, J. M., Jaffe, J. S. (in prep). BRDFs of deep sea creatures: Measurements and models.

Haag, J. M., Sweeney, A. M., and Jaffe, J. S. (2012). Measurement system for obtaining marine animal reflectance functions. *Proceedings of Ocean Optics XXI Conference*, Glasgow, Scotland, United Kingdom, October 8-12, 2012.

Holt, A.L., Wehner, J.G.A., Hampp, A., and Morse, D.E. (2010). Plastic transmissive infrared electrochromic devices. *Macromolecular Chemistry and Physics* **211**: 1701-1707.

Holt, A.L.., Sweeney, A.M., Johnsen, S., and Morse, D.E. (2011). A highly-distributed Bragg stack with unique geometry provides effective camouflage for Loligo squid eyes. *Journal of the Royal Society: Interface* **8,** 1386-1399.

Holt, A.L., Vahidinia, S., Gagnon, Y., Morse, D.E., and Sweeney, A.M., Iridocytes enhance radiative transfer in tridacnid clam photosymbiosis. In review at *Science*

Izumi, M., A. M. Sweeney, D. G. DeMartini, J. C. Weaver, M. L. Powers, A.R. Tao, T. V. Silvas, R. M. Kramer, W. J. Crookes-Goodson, L. M. Mäthger, R. R. Naik, R. T. Hanlon and Morse, D. E. (2010). Changes in reflectin protein phosphorylation are associated with dynamic iridescence in squid. *Journal of the Royal Society: Interface* **7**: 549-560.

Jaffe, J. S., Simonet, F., Laxton, B., Roberts, P. L. D., Zylinski, S., Johnsen, S., and A. Sweeney (in review). Omni-Cam and the Sub Sea Holodeck: Systems for recording *in-situ* radiance and simulating underwater optical environments in the lab. *Mar. Tech. Soc. J.*

Jaffe, J. S., Laxton, B., Zylinski, S. (2011). Omni-Cam and the Sub Sea Holodeck: Systems for recording *in-situ* radiance and simulating underwater optical environments in the lab. Proc. IEEE Oceans Conf., Santander, Spain June 6-9, 2011.

Johnsen, S., Marshall, N. J., and Widder, E. A. (2011). Polarization sensitivity as a contrast enhancer in pelagic predators: Lessons from *in situ* polarization imaging of transparent zooplankton. *Philosophical Transactions of the Royal Society of London, Series B.* **366**: 655–670.

Johnsen, S., Gassmann, E., Reynolds, R. A., Mobley, C. D., and Stramski, D. (in prep). The asymmetry of the underwater light field and its implications for animal camouflage.

Johnsen, S., Marshall, N. J., and T. W. Cronin (in prep). Through the looking glass: Polarization vision versus transparency and mirror-based camouflage in the open sea.

Johnsen, S. (2013). Hide and seek in the open sea: Pelagic camouflage and visual countermeasures. *Annual Review of Marine Science* **9**, (corrected proofs on-line).

Li, L., Stramski, D., and Reynolds, R. A. Radiative transfer simulations of the solar light field within the ocean mesopelagic zone (in review). *Applied Optics*.

Li, Z., Zhang, Y., Holt, A.L., Kolasa, B.P., Wehner, J.G., Hampp, A., Bazan, B.C., Nguyen, T., and Morse, D.E. Electrochromic devices and thin film transistors from a new family of ethylenedioxythiophene based conjugated polymers. *New Journal of Chemistry* **35**: 1327-1334.

Marshall, N. J., and Johnsen, S. (2011). Camouflage in Marine fish. In *Animal Camouflage: Current issues and new perspectives*. Cambridge University Press: Cambridge UK.

Nilsson, D. E., Warrant, E. J., Johnsen, S., Hanlon, R. T., and N. Shashar (2012). A unique advantage for giant eyes in giant squid. *Current Biology* **22**, 683-688.

Nilsson, D. E., Warrant, E. J., Johnsen, S., Hanlon, R. T., and N. Shashar (in press). The giant eyes of giant squid are indeed unexpectedly large, but not if used for spotting sperm whales. *BMC Evolutionary Ecology*.

Nilsson, D. E., Warrant, E. J., and S. Johnsen (in press). Computational visual ecology in the pelagic realm. *Philosophical Transactions of the Royal Society of London, Series B.*

Sawicka, E., Stramski, D., Darecki, M., and Dubranna, J. (2012). Power spectral analysis of wave-induced fluctuations in downward irradiance within the near-surface ocean under sunny conditions. *Ocean Optics XXI*, Glasgow, Scotland. Program & Abstracts, p. 133-134.

Sweeney, A., Johnsen, S., A. Holt and D.E. Morse (in prep). Natural camouflage in the infrared? Predators and prey in the ocean's far-red Raman glow.

Sweeney, A.M., G. E. Clague, M. Baum, D.G. DeMartini, and D.E. Morse (in prep). Discovery of a reflectin-transglutaminase fusion protein in photonic cephalopod tissues.

Tao, A.R., D. G. DeMartini, M. Izumi, A. M. Sweeney, and Morse, D. E. (2010). The role of protein assembly in dynamically tunable bio-optical tissues. *Biomaterials* **31**:793-801

Zylinski, S., and Osorio, D. (2011). What can camouflage tell us about non-human visual perception? A case study of the cuttlefish. In *Animal Camouflage: Current issues and new perspectives*. Cambridge University Press: Cambridge UK.

Zylinski, S. How, M., Osorio, D., Hanlon, R. T., and Marshall, N. J. (2011). To be seen or to hide: visual characteristics of body patterns for camouflage and communication in the Australian giant cuttlefish, *Sepia apama*. *American Naturalist.*

Zylinski, S. and S. Johnsen (2012) Camouflage without compromise: Mesopelagic cephalopods switch between transparency and pigmentation to optimize camouflage in the deep. *Current Biology* **21,** 1937-1941.

Zylinski, S., A.-S. Darmaillacq, & N. Shashar (2012). Visual interpolation for contour completion by the European cuttlefish (*Sepia officinalis*) and its use in dynamic camouflage. *Proceedings of the Royal Society B: Biological Sciences* **276**: 3963-3969.

Zylinski, S. and S. Johnsen (in press). Visual cognition in deep-sea cephalopods: what we don't know and why we don't know it. *In*: Cephalopod Cognition, Editors: S. Darmaillacq and J. Mather.

Zylinski, S. and D. Osorio (in press). Cuttlefish camouflage: Vision and cognition. *In*: Cephalopod Cognition, Editors: S. Darmaillacq and J. Mather.

Zylinski, S., Gagnon, Y., Gross, T., Wheeler, J. and Johnsen, S. (in prep.). *Octopus bimaculoides* substrate choice: hierarchy and interactions between visual and tactile information.